Radiology

# Pediatric Chest Radiographic and CT Findings of Electronic Cigarette or Vaping Product Use–associated Lung Injury (EVALI)

*Maddy Artunduaga, MD • Devika Rao, MD • Jonathan Friedman, MD • Jeannie K. Kwon, MD • Cory M. Pfeifer, MD, MPH, MS • Amy Dettori, MD • Abbey J. Winant, MD • Edward Y. Lee, MD, MPH*

From the Pediatric Radiology Division, Department of Radiology (M.A., J.F., J.K.K., C.M.P.) and the Pediatric Respiratory Medicine Division, Department of Pediatrics (D.R., A.D.), UT Southwestern Medical Center and Children's Medical Center, 5323 Harry Hines Blvd, CMC F1.02, Dallas, TX 75390; and Department of Radiology, Boston Children's Hospital and Harvard Medical School, Boston, Mass (A.J.W., E.Y.L.). Received December 18, 2019; revision requested December 26; final revision received January 25, 2020; accepted January 28. **Address correspondence to** M.A. (e-mail: *maddy.artunduaga@utsouthwestern.edu*).

Conflicts of interest are listed at the end of this article.

**Radiology 2020; 295:430–438 • https://doi.org/10.1148/radiol.2020192778 • Content codes: CH PD**

***Background:*** Electronic cigarette or vaping product use–associated lung injury (EVALI) is a serious public health concern with substantial morbidity and mortality, particularly in young individuals.

***Purpose:*** To evaluate chest radiographic and chest CT findings of EVALI in the pediatric population.

***Materials and Methods:*** This was a retrospective study of children who presented to a tertiary pediatric hospital from December 2018 to December 2019. Patients fulfilled the Centers for Disease Control and Prevention criteria for EVALI and had chest radiographs and CT images available at initial presentation. Two pediatric radiologists independently reviewed imaging for pattern, distribution, and extent of pulmonary abnormalities, as well as for extrapulmonary abnormalities. Clinical information, management, and outcomes were reviewed. Interobserver agreement was measured with Cohen κ coefficient.

***Results:*** Seven male patients (50%) and seven female patients (50%) (mean age, 16 years; range, 13–18 years) were evaluated. All patients underwent chest radiography and CT within 4 days of presentation (range, 0–4 days). Chest radiographic findings included ground-glass opacity in 14 of 14 (100%) and consolidation in eight of 14 (57%). CT findings included ground-glass opacity in 14 of 14 (100%), consolidation in nine of 14 (64%), and interlobular septal thickening in two of 14 (14%). At CT, subpleural sparing was seen in 11 of 14 (79%) and a reversed halo sign was seen in five of 14 (36%). Chest radiographic and CT abnormalities were predominately bilateral in 14 of 14 (100%) and symmetric in 13 of 14 (93%), with lower lobe predominance in seven of 14 (50%). Extent of abnormality was predominately diffuse at both chest radiography and CT. There was almost perfect interobserver agreement between two reviewers for detecting abnormalities on chest radiographs (κ = 0.99; 95% confidence interval: 0.97, 1.00) and CT (κ = 0.99; 95% confidence interval: 0.98, 1.00).

***Conclusion:*** In pediatric patients, electronic cigarette or vaping product use–associated lung injury is characterized by bilateral symmetric ground-glass opacities, consolidation, and a lower lobe predominance at CT.

© RSNA, 2020

Electronic cigarettes (hereafter, e-cigarettes), also known as *vapes*, are battery-powered devices that aerosolize substances including flavors, tetrahydrocannabinol, and/or nicotine for inhalation. First introduced in the United States around 2007, e-cigarettes have become the most commonly used tobacco product among the U.S. youth since 2014, and e-cigarette use has continued to increase substantially among adolescents in the past few years (1).

Beginning in 2012, several case reports emerged raising the possibility of the link between e-cigarette use and lung injury (2–8). As of January 14, 2020, there have been 2668 reported cases with 60 confirmed deaths due to e-cigarette or vaping product use–associated lung injury (EVALI) in the U.S. territory, with patients under 18 years of age accounting for 15% of reported hospitalizations due to EVALI (9). The Centers for Disease Control and Prevention, or CDC, and the Food and Drug Administration, along with local and state departments and clinicians, have been actively researching the causes and pathophysiology of EVALI (9).

Imaging plays a crucial role in the initial detection and evaluation of progression of EVALI. In the adult population, case reports and series have described the clinical and imaging findings of EVALI (1,10–13). To our knowledge, there is currently no published information regarding the chest radiographic and CT findings in pediatric patients with EVALI. This population is particularly vulnerable to e-cigarette use and its potentially life-threatening consequences. The purpose of our study was to evaluate chest radiographic and CT findings of EVALI in the pediatric population.

## Materials and Methods

### Institutional Review Board Approval

This retrospective study of patients' chest radiographs, CT images, and medical records was approved by the investigators' institutional review board. Informed consent was waived due to the retrospective nature of this study. Patient confidentiality was maintained in accordance

This copy is for personal use only. To order printed copies, contact *reprints@rsna.org*

## Abbreviations

CI = confidence interval, EVALI = electronic cigarette or vaping product use–associated lung injury


## Summary

Chest imaging findings of electronic cigarette or vaping product use–associated lung injury (EVALI) in pediatric patients were bilateral symmetric ground-glass opacities with subpleural sparing, consolidation, and lower lobe predominance.

## Key Results

- The imaging findings of electronic cigarette or vaping product use–associated lung injury (EVALI) in pediatric patients were bilateral (14 of 14, 100%) and symmetric (13 of 14, 93%) ground-glass opacities, often with consolidation (nine of 14, 64%) and lower lobe predominance (seven of 14, 50%).
- Subpleural sparing of pulmonary abnormalities at CT was frequently present (11 of 14, 79%).
- The reversed halo sign (atoll sign) was found at CT (five of 14, 36%) in pediatric patients with EVALI.


with Health Insurance Portability and Accountability Act guidelines.

### Patient Population

Computerized search of the radiology department database at Children's Medical Center of Dallas was performed to identify consecutive pediatric patients (up to 18 years of age) from December 2018 to December 2019. Discussion with the pulmonology team was also performed to ensure that all clinically known patients diagnosed with EVALI potentially missed by computerized search were included in our study. All patients fulfilled both of the following inclusion criteria: met the CDC criteria for EVALI (9) and had chest radiographs and CT images available at initial presentation (9,14) (Table 1).

Information reviewed from the electronic medical record included patient demographics, e-cigarette and/or vaping use, and clinical presentation.

### Imaging Technique

***Chest radiographic technique.***—Anteroposterior projection radiographs ($n$ = 10) were obtained with mobile radiography equipment (Shimadzu, Nakagyo-ku, Kyoto, Japan) by using high voltage, tube current, and exposure times at a 100-cm focus-film distance. Posteroanterior and lateral projection radiographs ($n$ = 4) were obtained with nonportable radiography equipment (Shimadzu or Siemens Healthineers, Malvern, Pa) by using high voltage, tube current, and exposure times at a 180-cm focus-film distance.

***CT technique.***—Chest CT examinations were performed by using a dual-source multidetector CT scanner (Somatom Definition Flash; Siemens). For chest CT examinations performed with intravenous contrast medium, nonionic contrast medium (320 milligrams of iodine per milliliter) at a contrast dose of 2 mL/kg (not to exceed 4 mL/kg or 125 mL) was used. The area of coverage included the entire lungs from the thoracic inlet to the level of the diaphragm. With the patient in the supine position, CT images were obtained in a single breath hold at end inspiration. CT parameters included 0.6-mm collimation with weight-based low-dose tube current and kilovoltage, high-speed mode, and a pitch equivalent of 2.8. The raw data set was reconstructed at a slice thickness of 2 mm for routine chest CT. For thin-section CT and CT angiography, the raw data set was reconstructed at a slice thickness of 1 mm.

### Imaging Study Review

Two pediatric fellowship-trained radiologists (M.A. and A.J.W. [subspecialty-certified in pediatric radiology], each with 7 years of experience in interpreting pediatric chest radiographs and CT images) reviewed all chest radiographs and CT images independently in random order. Reviewers were aware that patients were suspected of having EVALI on the basis of clinical signs and symptoms. However, they were blinded to all other clinical information including whether the patients met the CDC criteria for EVALI, prior imaging studies and their reports, and the original reports of chest radiographs and CT images included in this study. A third pediatric radiology fellowship-trained and subspecialty-certified reviewer (E.Y.L., with 20 years of experience in interpreting pediatric chest imaging studies) served as the arbitrator. The third reviewer made the final decision when there was a discrepancy in reaching a consensus decision between the chest radiographic and CT findings of the two initial reviewers. The third reviewer had no knowledge of the findings and interpretations of the other two reviewers.

All chest radiographs and CT images were evaluated by using a picture archiving and communication system (Smart CR; Fujifilm Medical System, Stamford, Conn). For CT, images were evaluated by using standard lung (level, –700 HU; width, 1400–1500 HU) and soft-tissue (level, 40–50 HU; width, 400–450 HU) window settings. During evaluation, reviewers could also manually alter window level and width settings and zoom into areas of interest. Multiplanar reformats (eg, coronal and sagittal) of CT images were also used routinely for reviewer's evaluation of EVALI.

A total of seven noncontrast and seven contrast material–enhanced chest CT examinations were performed. Of those, four CT examinations were performed in outside institutions. Overall, four CT examinations were performed with thin-section CT protocol, eight CT examinations were performed with routine chest CT protocol, and two CT examinations were performed with CT angiography protocol.

***Chest radiographic review.***—The reviewers systematically reviewed chest radiographs for abnormalities in the lung parenchyma, airways, pleura, and mediastinum based on the established criteria, as described in the following sections.

**Evaluation of Lung Parenchyma and Airways.**—Lung parenchyma and airway were evaluated for peribronchial markings, ground-glass opacity, consolidation, nodular opacity, and reticular markings. The presence of prominent peribronchial marking was diagnosed when coarse linear markings were

identified radiating from the hilar region into the lungs (15). The diagnosis of ground-glass opacity was made when there was a hazy area of increased opacity without obscuration of the underlying vessels and airway walls (16). Consolidation was diagnosed when there was an area of increased opacity that obscured the margins of vessels and airway walls, with or without air bronchogram(s) (16). The diagnosis of nodular opacity was made when a focal round opacity was present (16). Reticular opacity was diagnosed when linear opacities forming a mesh-like pattern were detected (16).

When lung parenchymal and airway abnormalities were present, they were also evaluated for the anatomic distribution and extent of abnormality. The anatomic distribution of the lung parenchyma and airway abnormalities was categorized as follows: unilateral or bilateral; predominantly central or peripheral; involvement of upper, middle, or lower lung zone (based on each zone comprising a third of the craniocaudal extent of the lungs on the frontal radiograph); and focal or multifocal (more than one focus of abnormalities). When bilateral involvement was present, the involvement of lung parenchymal and airway abnormalities was further classified as either symmetric or asymmetric. The extent of lung parenchymal and airway abnormalities was graded visually as the percentage of each lung involved in quartiles (0%–25%, 25%–50%, 50%–75%, 75%–100%), and an average was calculated for both lungs.

**Table 1: Summary of CDC Surveillance Case Criteria Definition for Severe Pulmonary Disease Associated with Electronic Cigarette or Vaping Product Use–associated Lung Injury (EVALI)**

| |
|---|
| 1. Electronic (e-cigarette) use or dabbing (superheated aerosol inhalation of substances with high THC concentration) during the 90 days before symptom onset |
| 2. Pulmonary opacities at chest radiography or ground-glass opacities at chest CT |
| 3. Absence of pulmonary infection on initial work-up (after minimum criteria met) OR infection identified with culture, polymerase chain reaction, or minimum criteria not met (testing not performed), but the clinical team believes this infection is not the sole cause of the underlying lung injury. |
| 4. No clinical evidence in the medical record of plausible alternative diagnoses (eg, cardiac, rheumatologic, or neoplastic process) |

Note.—CDC = Centers for Disease Control and Prevention, THC = tetrahydrocannabinol. Source.—Reference 9.

**Table 2: Summary of Patient Demographics in Pediatric Patients with Electronic Cigarette or Vaping Product Use–associated Lung Injury (EVALI)**

| | Demographics | | Electronic Cigarette or Vaping Product Used | | | |
|---|---|---|---|---|---|---|
| Patient No. | Age (y) | Sex | THC | THC and Nicotine | Nicotine | Time between Symptom Onset and Imaging |
| 1 | 16 | Female | | Yes | | 1 day |
| 2 | 15 | Male | Yes | | | 5 days |
| 3 | 17 | Male | Yes | | | 8 days |
| 4 | 16 | Male | | Yes | | 1.5 weeks |
| 5 | 14 | Female | | | Yes | 2 weeks |
| 6 | 17 | Female | Yes | | | 4 weeks |
| 7 | 13 | Male | Yes | | | 1 day |
| 8 | 17 | Male | Yes | | | 1 week |
| 9 | 16 | Female | | Yes | | 5 days |
| 10 | 16 | Male | Yes | | | 5 days |
| 11 | 16 | Female | Yes | | | 1.5 weeks |
| 12 | 17 | Female | | Yes | | 3 days |
| 13 | 16 | Female | Yes | | | 3 weeks |
| 14 | 17 | Male | Yes | | | 2.5 weeks |

Note.—THC = tetrahydrocannabinol.

**Evaluation of Pleura and Mediastinum.**—Pleural and mediastinal abnormalities were noted (16).

*Chest CT review.*—After chest radiographic evaluation, chest CT images were rerandomized to minimize reviewer bias. Then, the reviewers systematically assessed chest CT images for abnormalities in the lung parenchyma, airways, pleura, mediastinum, and vascular structures based on the established criteria, as described in the following sections (16).

**Evaluation of Lung Parenchyma and Airway.**—Lung parenchyma and airway were evaluated for ground-glass opacity (diffuse vs centrilobular nodular pattern), consolidation, nodule(s), bronchiectasis, cyst(s), and interlobular septal thickening. The diagnosis of ground-glass opacity was made when hazy increased attenuation of lung, with preservation of the bronchial and vascular margins, was present (16). When ground-glass opacity was present, it was assessed as having either diffuse or centrilobular ground-glass nodular pattern. The diagnosis of consolidation was made when a homogeneous increase in pulmonary parenchymal attenuation, obscuring the margins of vessels and airway walls, was present (16). When a rounded or irregular opacity measuring up to 3 cm in diameter was present, the diagnosis of a nodule was made (16). Bronchiectasis was diagnosed when there was bronchial dilatation with respect to the accompanying pulmonary artery, lack of tapering of bronchi, and identification of bronchi within 1 cm of the pleural surface (16). The diagnosis of cyst or cysts was made when there was a round parenchymal low-attenuation area with a well-defined interface with normal lung and without a central area of vasculature to suggest the presence of centrilobular emphysema (16). The diagnosis of the interlobular septal thickening was made when thin linear opacities at

**Table 3: Chest Radiographic Findings of Pediatric Patients with Electronic Cigarette or Vaping Product Use–associated Lung Injury (EVALI)***

| | Parenchymal Abnormalities* | | | | |
|---|---|---|---|---|---|
| Patient No. | Ground-Glass Opacity | Consolidation | Lobar Involvement | Lobar Predominance | Extent (%) |
| 1 | Yes | Yes | RUL, RML, RLL, LUL, LIN, LLL | | >75 |
| 2 | Yes | Yes | RUL, RML, RLL, LUL, LIN, LLL | | 50–75 |
| 3 | Yes | | RUL, RML, RLL, LUL, LIN, LLL | | 25–50 |
| 4 | Yes | | RUL, RML, RLL, LUL, LIN, LLL | LL | 25–50 |
| 5 | Yes | Yes | RUL, RML, RLL, LUL, LIN, LLL | | >75 |
| 6 | Yes | | RUL, RML, RLL, LUL, LIN, LLL | LL | <25 |
| 7 | Yes | Yes | RUL, RML, RLL, LUL, LIN, LLL | LL | 50–75 |
| 8 | Yes | | RUL, RML, RLL, LUL, LIN, LLL | | 50–75 |
| 9 | Yes | | RUL, RML, RLL, LUL, LIN, LLL | LL | 25–50 |
| 10 | Yes | Yes | RUL, RML, RLL, LUL, LIN, LLL | | >75 |
| 11 | Yes | | RUL, RML, RLL, LUL, LIN, LLL | LL | 25–50 |
| 12 | Yes | Yes | RUL, RML, RLL, LUL, LIN, LLL | | >75 |
| 13 | Yes | Yes | RUL, RML, RLL, LUL, LIN, LLL | LL | 50–75 |
| 14 | Yes | Yes | RUL, RML, RLL, LUL, LIN, LLL | LL | 50–75 |

Note.—LIN = lingula, LL = lower lobe, LLL = left lower lobe, LUL = left upper lobe, RLL = right lower lobe, RML = right middle lobe, RUL = right upper lobe.

* All patients had symmetric parenchymal abnormalities except patient 12 (left less than right involvement). Additionally, patient 3 had a pneumothorax; patient 5 had a pleural effusion.

right angles to and in contact with the lateral pleural surfaces near the lung bases were present (16).

When lung parenchymal and airway abnormalities were present, they were also evaluated for the anatomic distribution and extent of abnormality. The anatomic distribution of the lung parenchyma and airway abnormalities was categorized as follows: unilateral or bilateral, predominantly central or peripheral, involvement of six lobes (right upper lobe, right middle lobe, right lower lobe, left upper lobe, lingula, and left lower lobe), and focal or multifocal (more than one lobe involvement). When lung parenchymal and airway abnormalities were bilateral, they were further classified as either symmetric or asymmetric. In cases where lung parenchymal and airway abnormalities were peripherally located, the presence of associated subpleural sparing of abnormalities was also evaluated. The diagnosis of a reversed halo sign (atoll sign) was defined as the presence of a central ground-glass opacity surrounded by denser consolidation of crescentic shape (forming more than three-fourths of a circle) or complete ring of at least 2-mm thickness (16). For assessing the extent of lung parenchymal and airway abnormalities, it was graded visually as the percentage of each lobe involved, and an average was calculated for both lungs. Estimated involvement was divided into quartiles (0%–25%, 25%–50%, 50%–75%, 75%–100%).

**Evaluation of Pleura and Mediastinum.**—Pleural and mediastinal abnormalities were also recorded. Lymphadenopathy was recorded when the short-axis diameter of mediastinal nodes was larger than 1 cm at chest CT (16).

**Evaluation of Vascular Structures.**—Thoracic vascular structures were evaluated for the presence of pulmonary embolism in one of seven CT images (14.3%) obtained with intravenous contrast medium. The presence of pulmonary embolism was defined as either a complete or partial low-attenuation filling defect in a pulmonary artery (17–19).

***Evaluation of CT Findings Based on American Thoracic Society and European Respiratory Society Classification of the Idiopathic Interstitial Pneumonia.***—The constellation of the lung findings on CT images in each patient was categorized into a pattern based the American Thoracic Society and European Respiratory Society Classification of the Idiopathic Interstitial Pneumonias (13,20).

## Statistical Analysis

Normally distributed continuous variables (eg, age and interval between the date of initial chest radiographs and chest CT examinations) were expressed as the mean ± standard deviation and range. The percentage of the presence of abnormalities seen in the lung parenchyma and airway, pleura, and mediastinum on the chest radiographs and chest CT images was calculated.

Agreement between reviewers was assessed by using the κ statistic with 95% confidence intervals (CIs). Interpretation of the strength of agreement beyond chance level is based on the Landis and Koch benchmarks (κ values: 0–0.20, slight agreement; 0.21–0.40, fair agreement; 0.41–0.60, moderate agreement; 0.61–0.80, substantial agreement; 0.81–1.00, almost perfect agreement) (21,22). Statistical analysis was performed by using

the SPSS software package (version 18.0; SPSS, Chicago, Ill).

## Results

### Patient Cohort

The patient population consisted of seven male and seven female patients (mean age ± standard deviation, 16 years ± 1; range, 13–18 years) (Table 2). All patients included in this study used an e-cigarette or engaged in *dabbing* (superheated aerosol inhalation of substances with high tetrahydrocannabinol concentration) in the 90 days before symptom onset. Fifteen patients with a history of vaping were excluded because they had normal chest radiographic findings without CT examinations performed, and they did not meet CDC criteria for the diagnosis of EVALI. Four of 14 patients (29%) had a history of exposure to both tetrahydrocannabinol- and nicotine-containing vaping products. Nine of 14 patients (64%) had a history of exposure to tetrahydrocannabinol-containing vaping products only. One of 14 patients (7%) had a history of exposure to nicotine-containing vaping products only.

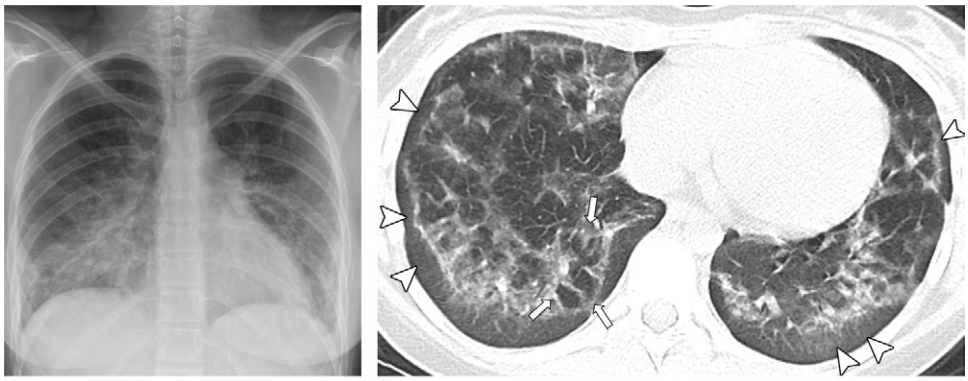


**Figure 1:** Images in a 16-year-old girl with history of electronic cigarette product use for 1 year and tetrahydrocannabinol dabbing for 2 months who presented with cough, weight loss, nausea, and vomiting for 3 weeks. **(a)** Posteroanterior digital chest radiograph from day of presentation shows bilateral symmetric ground-glass opacities with consolidation and lower lobe predominance. **(b)** Axial lung window (width, 1500; level, –700) image of noncontrast chest CT performed on day of presentation demonstrates bilateral ground-glass opacities with subpleural sparing (arrowheads) and reversed halo sign (atoll sign) (arrows) in right lower lobe.

All 14 patients (100%) included in this study had respiratory symptoms including shortness of breath (12 of 14, 86%), cough (12 of 14, 86%), chest pain (10 of 14, 71%), dyspnea on exertion (six of 14, 43%), and increased work of breathing (six of 14, 43%) (Table 2). Twelve patients (86%) also had gastrointestinal symptoms including vomiting (12 of 14, 86%), nausea (10 of 14, 71%), diarrhea (nine of 14, 64%), and abdominal pain (six of 14, 43%). Of note, four patients (29%) initially presented with isolated gastrointestinal symptoms and later developed respiratory symptoms after hospital admission. Constitutional symptoms were present in 13 (93%) patients including fever (12 of 14, 86%), weight loss (six of 14, 43%), fatigue (six of 14, 43%), and chills (three of 14, 21%).

### Imaging Findings

All patients had available chest radiographs and CT images acquired within 4 days of presentation (mean, 0 days; range, 0–4 days).

***Chest radiographic findings.***—Chest radiographic findings include ground-glass opacity in 14 patients (100%) and consolidation in eight patients (57%) (Table 3, Fig 1a). Radiographic abnormalities were almost always bilateral in 14 of 14 (100%) and symmetric in 13 of 14 (93%), with lower lobe predominance seen in seven patients (50%). The extent of abnormality was greater than 75% in four patients (29%), 50%–75% in five patients (36%), 25%–50% in four patients (29%), and less than 25% in one patient (7%). Extrapulmonary findings on chest radiographs included pneumomediastinum and bilateral small pleural effusions that were seen in one patient (7%) each.

***Chest CT findings.***—CT findings included ground-glass opacity in 14 patients (100%), consolidation in nine patients (64%), and interlobular septal thickening in two patients (14%) (Table 4, Fig 1b). Two patients (14%) with ground-glass opacity showed centrilobular ground-glass nodular pattern. CT abnormalities were predominately bilateral in 14 of 14 (100%) and symmetric in 13 of 14 (93%), with lower lobe predominance in seven patients (50%). Subpleural sparing was seen in 11 patients (79%) and a reversed halo sign (atoll sign) was seen in five patients (36%) (Figs 2, 3). The extent of abnormality was greater than 75% in 10 patients (71%), 50%–75% in two patients (14%), and less than 25% in two patients (14%). Extrapulmonary findings on CT images included pneumomediastinum in two patients (14%), bilateral small pleural effusions in one patient (7%), and pulmonary embolism in one patient (7%).

***Interobserver agreement.***—Among all 448 evaluations (196 evaluations for chest radiography and 252 evaluations for CT) between two reviewers, discrepancies between the two reviewers' interpretations occurred in two (0.45%) cases. The findings in question included the difference in the extent (25%–50% vs 50%–75%) of pulmonary abnormality on the chest radiograph in one case and a small pneumomediastinum on the CT image in the other case. The arbitrator assessed these two cases independently and determined that the extent of abnormality at chest radiography was 25%–50% and that there was a small pneumomediastinum at CT. Therefore, there was almost perfect interobserver agreement between two reviewers for detecting abnormalities on chest radiographs ($\kappa$ = 0.99; 95% CI: 0.97,1.00) and CT images ($\kappa$ = 0.99; 95% CI: 0.98, 1.00).

**Table 4: Chest CT Findings in Pediatric Patients with Electronic Cigarette or Vaping Product Use–associated Lung Injury (EVALI)***

| | Type of Parenchymal Abnormalities | | | | Pattern of Abnormalities | | Distribution | | | Extent (%) | | | | |
|---|---|---|---|---|---|---|---|---|---|---|---|---|---|---|
| Patient No. | GGO | Cons | CGGNO | IST | SS | Atoll | Diffuse | Lobar Involvement | Lobe Predominance | Upper | Mid | Lower | Specific Features | Overall Patterns |
| 1 | Yes | Yes | | | Yes | Yes | Yes | RUL, RML, RLL, LUL, LIN, LLL | | 25–50 | 25–50 | 25–50 | GGO, cons, atoll | COP |
| 2 | Yes | Yes | | | Yes | | Yes | RUL, RML, RLL, LUL, LIN, LLL | | >75 | >75 | >75 | GGO, cons | COP |
| 3 | Yes | Yes | | | Yes | Yes | Yes | RUL, RML, RLL, LUL, LIN, LLL | | >75 | >75 | >75 | GGO, cons, atoll | COP |
| 4 | Yes | | | | Yes | | Yes | RUL, RML, RLL, LUL, LIN, LLL | LL | >75 | >75 | >75 | GGO | HP |
| 5 | Yes | Yes | Yes | Yes | | | Yes | RUL, RML, RLL, LUL, LIN, LLL | | >75 | >75 | >75 | GGO, cons, CG-GNO, pl eff | AEP |
| 6 | Yes | | | | | | Yes | RUL, RML, RLL, LUL, LIN, LLL | LL | <25 | <25 | <25 | GGO | HP |
| 7 | Yes | | | | Yes | | Yes | RUL, RML, RLL, LUL, LIN, LLL | LL | <25 | <25 | <25 | GGO | HP |
| 8 | Yes | Yes | | | Yes | | Yes | RUL, RML, RLL, LUL, LIN, LLL | | >75 | >75 | >75 | GGO, cons | COP |
| 9 | Yes | | | Yes | | | Yes | RUL, RML, RLL, LUL, LIN, LLL | LL | 25–50 | >75 | >75 | GGO, CP | ALI (DAD) |
| 10 | Yes | Yes | | | Yes | Yes | Yes | RUL, RML, RLL, LUL, LIN, LLL | | 50–75 | 50–75 | 50–75 | GGO, cons, atoll | COP |
| 11 | Yes | | | | Yes | | Yes | RUL, RML, RLL, LUL, LIN, LLL | LL | >75 | >75 | >75 | GGO | HP |
| 12 | Yes | Yes | | | Yes | | Yes | RUL, RML, RLL, LUL, LIN, LLL | | >75 | >75 | >75 | GGO, cons | ALI (DAD) |
| 13 | Yes | Yes | | | Yes | Yes | Yes | RUL, RML, RLL, LUL, LIN, LLL | LL | 25–50 | 50–75 | >75 | GGO, cons, atoll | COP |
| 14 | Yes | Yes | Yes | | Yes | Yes | Yes | RUL, RML, RLL, LUL, LIN, LLL | LL | >75 | >75 | >75 | GGO, cons, CG-GNO, atoll | COP |

Note.— AEP = acute eosinophilic pneumonia, ALI = acute lung injury, atoll = reversed halo sign (atoll sign), CGGNO = centrilobular ground-glass nodular opacity, cons = consolidation, COP = cryptogenic organizing pneumonia, DAD = diffuse alveolar damage, GGO = ground-glass opacity, HP = hypersensitivity pneumonitis, IST = interlobular septal thickening, LIN = lingula, LL = lower lobe, LLL = left lower lobe, LUL = left upper lobe, pl eff = pleural effusion, RLL = right lower lobe, RML = right middle lobe, RUL = right upper lobe, SS = subpleural sparing of pulmonary abnormality.

* Additionally, patients 1 and 3 had a pneumothorax; patient 5 had a pleural effusion; patient 14 had a pulmonary embolism.

***CT Findings Based on American Thoracic Society and European Respiratory Society Classification of the Idiopathic Interstitial Pneumonias*—**The overall pattern of lung findings at CT in our pediatric study population included cryptogenic organizing pneumonia in seven patients (50%), hypersensitive pneumonitis in four patients (29%) (Fig 4a, 4b), acute lung injury (typically, diffuse alveolar hemorrhage histologically) in two patients (14%), and acute eosinophilic pneumonia in one patient (7%) (Table 4).

## Discussion

Our study found that electronic cigarette or vaping product use–associated lung injury (EVALI) in pediatric patients has characteristic chest radiographic and CT findings. Bilateral (14 of 14, 100%) and symmetric (13 of 14, 93%) ground-glass opacity, frequently associated with consolidation (nine of 14, 64%) and with lower lobe predominance (seven of 14, 50%), was the characteristic imaging finding in pediatric patients with EVALI. In addition, subpleural sparing (ie, the parenchymal abnormality not extending to the pleura) was visualized in the vast majority (79%) of patients. Another imaging feature, observed in 36% of our pediatric patients with EVALI, was the reversed halo sign (atoll sign), which is characterized by the presence of a central ground-glass opacity surrounded by denser consolidation of crescentic shape or complete ring.

Electronic cigarette (hereafter, e-cigarette) liquids and aerosols contain a variety of chemical constituents that can result in adverse health effects (23). Vitamin E acetate (a tetrahydrocannabinol-containing e-cigarette or vaping product additive) has been recently associated with this potentially fatal outbreak, as it has been found in analyzed bronchoalveolar lavages of patients with EVALI but not in healthy control participants throughout the nation (9,24). When these potentially harmful chemical constituents are inhaled, it is plausible that acute lung injury may occur. A previously published study based on lung biopsy specimens in patients with e-cigarette or vaping product use (25) demonstrated histologic features of acute lung injury, supporting the hypothesis that inhalation of e-cigarette aerosol can cause lung damage. Fibrous exudates within the alveoli (signifying the presence of substantial lung damage) seen at pathologic analysis may explain the ground-glass opacities that were observed at imaging in our study population. The preservation of subpleural regions of the lungs (also known as subpleural sparing) was a characteristic CT imaging feature in our study population with EVALI. We believe that such imaging finding may reflect the main involvement of the central aspect of the secondary pulmonary lobule in response to an inhaled agent.

The chest radiograph alone does not allow the sufficient characterization of the patterns of EVALI in pediatric patients, and therefore chest CT, which is associated with higher radiation dose than radiograph, may be necessary. Although pediatric chest radiography has an estimated effective dose of approximately 0.02 mSv and chest CT doses have been on the order of 3 mSv (26), recent advances in low-dose CT techniques have yielded diagnostic studies that have decreased the dose up to 93% (27). This benefit in dose reduction is particularly realized when CT is performed at children's hospitals, which

**Figure 2:** Image in a 16-year-old girl with history of chronic abdominal pain and electronic cigarette product use with nicotine and tetrahydrocannabinol for 1 year who presented with acute abdominal pain and vomiting 1 day prior to admission. Patient later developed shortness of breath and increased work of breathing. Axial lung window (width, 1500; level, –700) image of chest CT with contrast enhancement performed 1 day prior to admission shows presence of central ground-glass opacity surrounded by denser complete ring of consolidation, also known as the reversed halo sign (atoll sign) (arrows). Subpleural sparing (arrowheads) of lung abnormality is also seen.

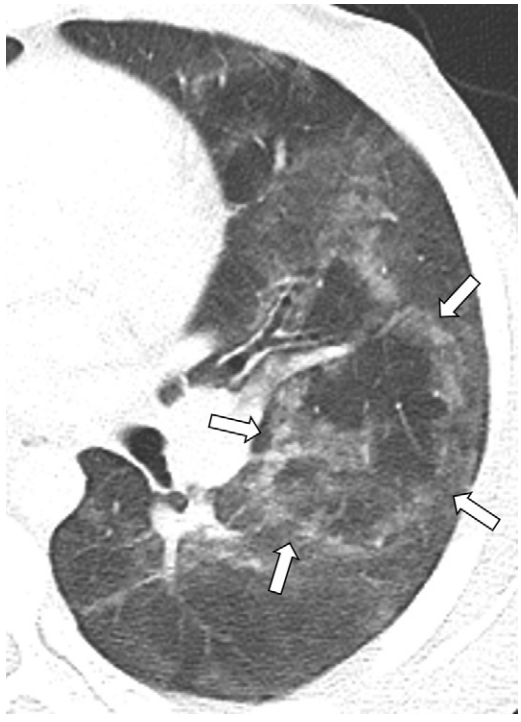

**Figure 3:** Image in a 17-year-old boy with history of electronic cigarette tetrahydrocannabinol use for 2 months presented with 8 days of nausea, vomiting, abdominal pain, and fever. Patient later developed shortness of breath and chest pain. Axial lung window (width, 1500; level, –700) image of CT with contrast enhancement performed 1 day after presentation demonstrates presence of central ground-glass opacity surrounded by complete ring of denser consolidation, also known as the reversed halo sign (atoll sign) (arrows).

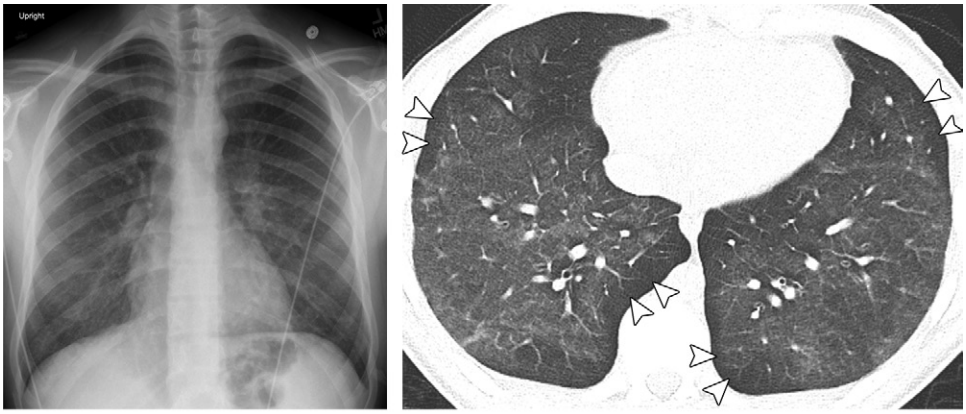


a. b.

**Figure 4:** Images in a 16-year-old boy with 2-year history of daily nicotine and tetrahydrocannabinol vaping presented with 1.5 weeks of cough, shortness of breath, nausea, and vomiting. **(a)** Posteroanterior digital chest radiograph from day of presentation shows bilateral symmetric ground-glass opacities with lower lobe predominance. **(b)** Axial lung window (width, 1500; level, –700) image of noncontrast chest CT performed 1 day after presentation demonstrates bilateral ground-glass opacities with subpleural sparing (arrowheads).

tend to use lower-dose techniques more broadly than do other hospitals (28). The radiation dose associated with CT is thus in line with the principles of ALARA ("As Low As Reasonably Achievable") and the Image Gently campaign, and is justified in the evaluation of pediatric patients suspected of having EVALI. We also found that in some cases, the initial symptoms may lead clinicians to suspect a gastrointestinal etiology for the patient's presentation, and the radiologist may be the first to suggest EVALI as a diagnostic consideration. In our cohort, pulmonary abnormalities were only first detected in three of four (75%) patients who had presented exclusively with gastrointestinal symptoms and had undergone initial abdomen and pelvis CT.

Although a variety of imaging findings have been reported in patients with EVALI, bilateral and lower lobe predominant ground-glass opacity and consolidation, often with areas of subpleural sparing, were the most common findings. The results of our study correlate well with the findings from previously published studies on EVALI (1–8,10–13). Interestingly, our study found that the reversed halo sign (atoll sign), another characteristic imaging finding, was seen in five of 14 (36%) pediatric patients with EVALI. Although it was initially thought to be specific for cryptogenic organizing pneumonia, which was the predominant overall pattern in 50% of our patient population (29), the reversed halo sign (atoll sign) is now known to be seen in a variety of pulmonary diseases during both early developing acute lung injury and also during resolution (30). The relationship between imaging, physiologic findings, and clinical findings in adults have been recently described (31,32).

There were several limitations in our study. First, the patient population was relatively small. Second, imaging techniques for chest radiography and chest CT were not standardized for all patients included in this study. Based on our study population, we cannot assess for appearance differences at CT that may allow discernable patterns between pure tetrahydrocannabinol and pure nicotine use because there was only one patient that reported nicotine-exclusive use. Lastly, we acknowledge that there was no pathologic correlation performed.

In conclusion, the results of our study suggest that the imaging findings of electronic cigarette or vaping product use–associated lung injury in pediatric patients are characterized by the presence of bilateral symmetric ground-glass opacity, with consolidation and often with a lower lobe predominance. At CT, subpleural sparing is frequently present, and the reversed halo sign (atoll sign) is a unique feature that may also be seen.

**Acknowledgments:** We would like to acknowledge medical student Kendra Maple and Dr Stephanie Hsu from the Pediatric Clinical Care Department for gathering clinical information and creating a database.

**Author contributions:** Guarantors of integrity of entire study, M.A., C.M.P.; study concepts/study design or data acquisition or data analysis/interpretation, all authors; manuscript drafting or manuscript revision for important intellectual content, all authors; approval of final version of submitted manuscript, all authors; agrees to ensure any questions related to the work are appropriately resolved, all authors; literature research, all authors; clinical studies, M.A., D.R., J.F., A.D., A.J.W., E.Y.L.; statistical analysis, M.A., D.R., C.M.P., E.Y.L.; and manuscript editing, M.A., D.R., J.F., J.K.K., C.M.P., A.J.W., E.Y.L.

**Disclosures of Conflicts of Interest: M.A.** disclosed no relevant relationships. **D.R.** disclosed no relevant relationships. **J.F.** disclosed no relevant relationships. **J.K.K.** disclosed no relevant relationships. **C.M.P.** disclosed no relevant relationships. **A.D.** disclosed no relevant relationships. **A.J.W.** disclosed no relevant relationships. **E.Y.L.** Activities related to the present article: disclosed no relevant relationships. Activities not related to the present article: provides medical legal consult to Cambridge Medical Experts and Expert Institute; received traveling support and honorarium from the Guerbet group as an invited speaker at an international meeting (Asian and Oceanic Society for Paediatric Radiology (AOSPR); receives royalties from Lippincott Williams & Wilkins. Other relationships: disclosed no relevant relationships.

## References

1. Abbara S, Kay FU. Electronic Cigarette or Vaping-associated Lung Injury (EVALI): The Tip of the Iceberg. Radiol Cardiothorac Imaging 2019;1(4):e190212.
2. McCauley L, Markin C, Hosmer D. An unexpected consequence of electronic cigarette use. Chest 2012;141(4):1110–1113.
3. Thota D, Latham E. Case report of electronic cigarettes possibly associated with eosinophilic pneumonitis in a previously healthy active-duty sailor. J Emerg Med 2014;47(1):15–17.
4. He T, Oks M, Esposito M, Steinberg H, Makaryus M. "Tree-in-Bloom": Severe Acute Lung Injury Induced by Vaping Cannabis Oil. Ann Am Thorac Soc 2017;14(3):468–470https://doi.org/10.1513/AnnalsATS.201612-974LE.
5. Khan MS, Khateeb F, Akhtar J, et al. Organizing pneumonia related to electronic cigarette use: A case report and review of literature. Clin Respir J 2018;12(3):1295–1299.
6. Sommerfeld CG, Weiner DJ, Nowalk A, Larkin A. Hypersensitivity Pneumonitis and Acute Respiratory Distress Syndrome From E-Cigarette Use. Pediatrics 2018;141(6):e20163927.
7. Arter ZL, Wiggins A, Hudspath C, Kisling A, Hostler DC, Hostler JM. Acute eosinophilic pneumonia following electronic cigarette use. Respir Med Case Rep 2019;27:100825.
8. Anderson RP, Zechar K. Lung injury from inhaling butane hash oil mimics pneumonia. Respir Med Case Rep 2019;26:171–173.

9. U.S. Centers for Disease Control and Prevention. Outbreak of Lung Injury Associated with E-Cigarette Use, or Vaping. https://www.cdc.gov/tobacco/basic_information/e-cigarettes/severe-lung-disease.html. Published 2019. Accessed December 29, 2019.
10. Henry TS, Kanne JP, Kligerman SJ. Imaging of Vaping-Associated Lung Disease. N Engl J Med 2019;381(15):1486–1487.
11. Sechrist JW, Kanne JP. Vaping-associated Lung Disease. Radiology 2020;294(1):18.
12. Layden JE, Ghinai I, Pray I, et al. Pulmonary Illness Related to E-Cigarette Use in Illinois and Wisconsin - Preliminary Report. N Engl J Med 2019 Sep 6 [Epub ahead of print].
13. Henry TS, Kligerman SJ, Raptis CA, Mann H, Sechrist JW, Kanne JP. Imaging Findings of Vaping-Associated Lung Injury. AJR Am J Roentgenol 20191–8.
14. Schier JG, Meiman JG, Layden J, et al. Severe Pulmonary Disease Associated with Electronic-Cigarette-Product Use - Interim Guidance. MMWR Morb Mortal Wkly Rep 2019;68(36):787–790.
15. Lee EY, McAdam AJ, Chaudry G, Fishman MP, Zurakowski D, Boiselle PM. Swine-origin influenza a (H1N1) viral infection in children: initial chest radiographic findings. Radiology 2010;254(3):934–941.
16. Hansell DM, Bankier AA, MacMahon H, McLoud TC, Müller NL, Remy J. Fleischner Society: glossary of terms for thoracic imaging. Radiology 2008;246(3):697–722.
17. Kritsaneepaiboon S, Lee EY, Zurakowski D, Strauss KJ, Boiselle PM. MDCT pulmonary angiography evaluation of pulmonary embolism in children. AJR Am J Roentgenol 2009;192(5):1246–1252.
18. Thacker PG, Lee EY. Pulmonary embolism in children. AJR Am J Roentgenol 2015;204(6):1278–1288.
19. Lee EY, Tse SK, Zurakowski D, et al. Children suspected of having pulmonary embolism: multidetector CT pulmonary angiography--thromboembolic risk factors and implications for appropriate use. Radiology 2012;262(1):242–251.
20. Travis WD, Costabel U, Hansell DM, et al. An official American Thoracic Society/European Respiratory Society statement: Update of the international multidisciplinary classification of the idiopathic interstitial pneumonias. Am J Respir Crit Care Med 2013;188(6):733–748.
21. Kundel HL, Polansky M. Measurement of observer agreement. Radiology 2003;228(2):303–308.
22. Landis JR, Koch GG. The measurement of observer agreement for categorical data. Biometrics 1977;33(1):159–174.
23. Floyd EL, Queimado L, Wang J, Regens JL, Johnson DL. Electronic cigarette power affects count concentration and particle size distribution of vaping aerosol. PLoS One 2018;13(12):e0210147.
24. Ellington S, Salvatore PP, Ko J, et al. Update: Product, Substance-Use, and Demographic Characteristics of Hospitalized Patients in a Nationwide Outbreak of E-cigarette, or Vaping, Product Use-Associated Lung Injury - United States, August 2019-January 2020. MMWR Morb Mortal Wkly Rep 2020;69(2):44–49.
25. Mukhopadhyay S, Mehrad M, Dammert P, et al. Lung Biopsy Findings in Severe Pulmonary Illness Associated With E-Cigarette Use (Vaping). Am J Clin Pathol 2020;153(1):30–39.
26. Brody AS, Frush DP, Huda W, Brent RL; American Academy of Pediatrics Section on Radiology. Radiation risk to children from computed tomography. Pediatrics 2007;120(3):677–682.
27. Nagayama Y, Oda S, Nakaura T, et al. Radiation dose reduction at pediatric CT: use of low tube voltage and iterative reconstruction. RadioGraphics 2018;38(5):1421–1440.
28. Agarwal S, Jokerst C, Siegel MJ, Hildebolt C. Pediatric emergency CT scans at a children's hospital and at community hospitals: radiation technical factors are an important source of radiation exposure. AJR Am J Roentgenol 2015;205(2):409–413.
29. Voloudaki AE, Bouros DE, Froudarakis ME, Datseris GE, Apostolaki EG, Gourtsoyiannis NC. Crescentic and ring-shaped opacities. CT features in two cases of bronchiolitis obliterans organizing pneumonia (BOOP). Acta Radiol 1996;37(6):889–892.
30. Godoy MC, Viswanathan C, Marchiori E, et al. The reversed halo sign: update and differential diagnosis. Br J Radiol 2012;85(1017):1226–1235.
31. Caporale A, Langham MC, Guo W, Johncola A, Chatterjee S, Wehrli FW. Acute Effects of Electronic Cigarette Aerosol Inhalation on Vascular Function Detected at Quantitative MRI. Radiology 2019;293(1):97–106.
32. Kligerman S, Raptis C, Larsen B, et al. Radiologic, Pathologic, Clinical, and Physiologic Findings of Electronic Cigarette or Vaping Product Use-associated Lung Injury (EVALI): Evolving Knowledge and Remaining Questions. Radiology 2020 Jan 28 [Epub ahead of print].